

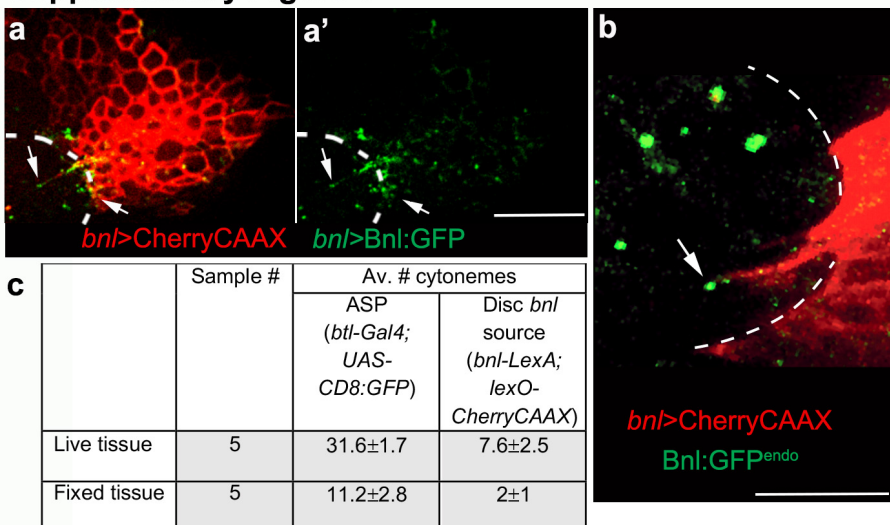
GPI-anchored FGF directs cytoneme-mediated bidirectional contacts to regulate its tissue-specific dispersion.

Lijuan Du, Alex Sohr, Yujia Li, Sougata Roy*

Contents

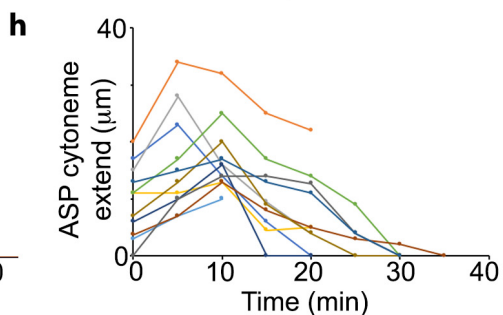
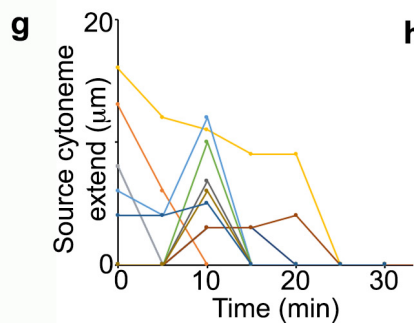
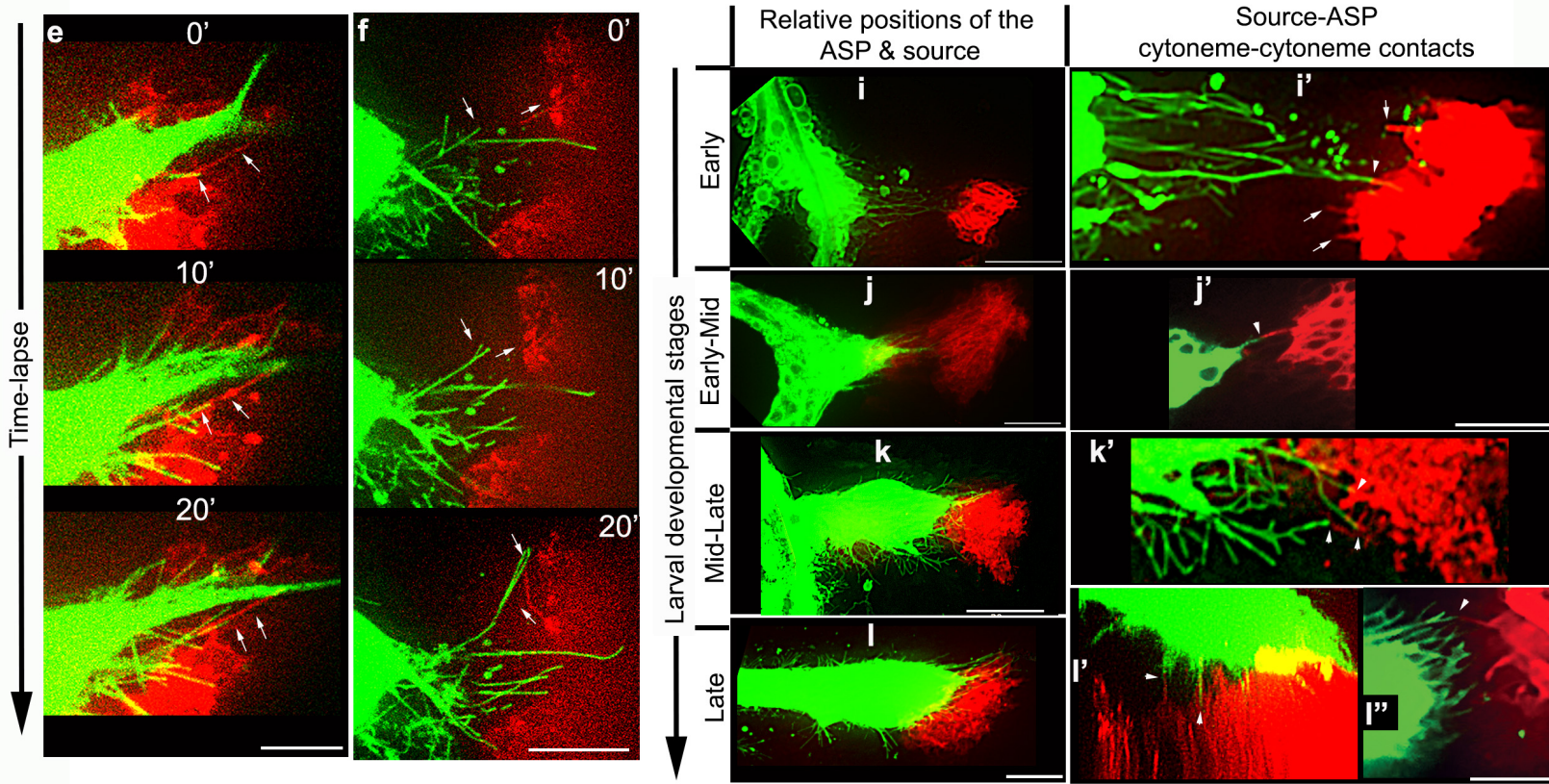
- 1. Supplementary Figures with Figure Legends (Suppl. Fig.1-Suppl. Fig.7)**
- 2. Supplementary Tables 1-4.**
- 3. Supplementary Notes:**
 - A. Expression analyses of *bnl* splice variants**
 - B. Bioinformatic analyses of physico-chemical properties of various constructs**
 - C. Comparison of *bnl-gal4*-driven expression of transgenic constructs**
 - D. Examples of gating strategy for FACS analyses**
- 4. Supplementary References**
- 5. R plot code**

Supplementary Figure 1



d	# of clones	# of cells in clones	# of cytonemes	# of cytonemes/cell
1	1	1	2	2
2	1	1	2	2
3	5	5	19	3.8
4	2	2	7	3.5
5	1	1	5	5
6	1	1	5	5
7	2	2	6	3
8	8	8	20	2.5
9	2	2	16	8
10	2	2	2	1
11	2	2	7	3.5
12	2	2	5	2.5
13	1	1	8	8
Average	2.3	2.3	8	3.8

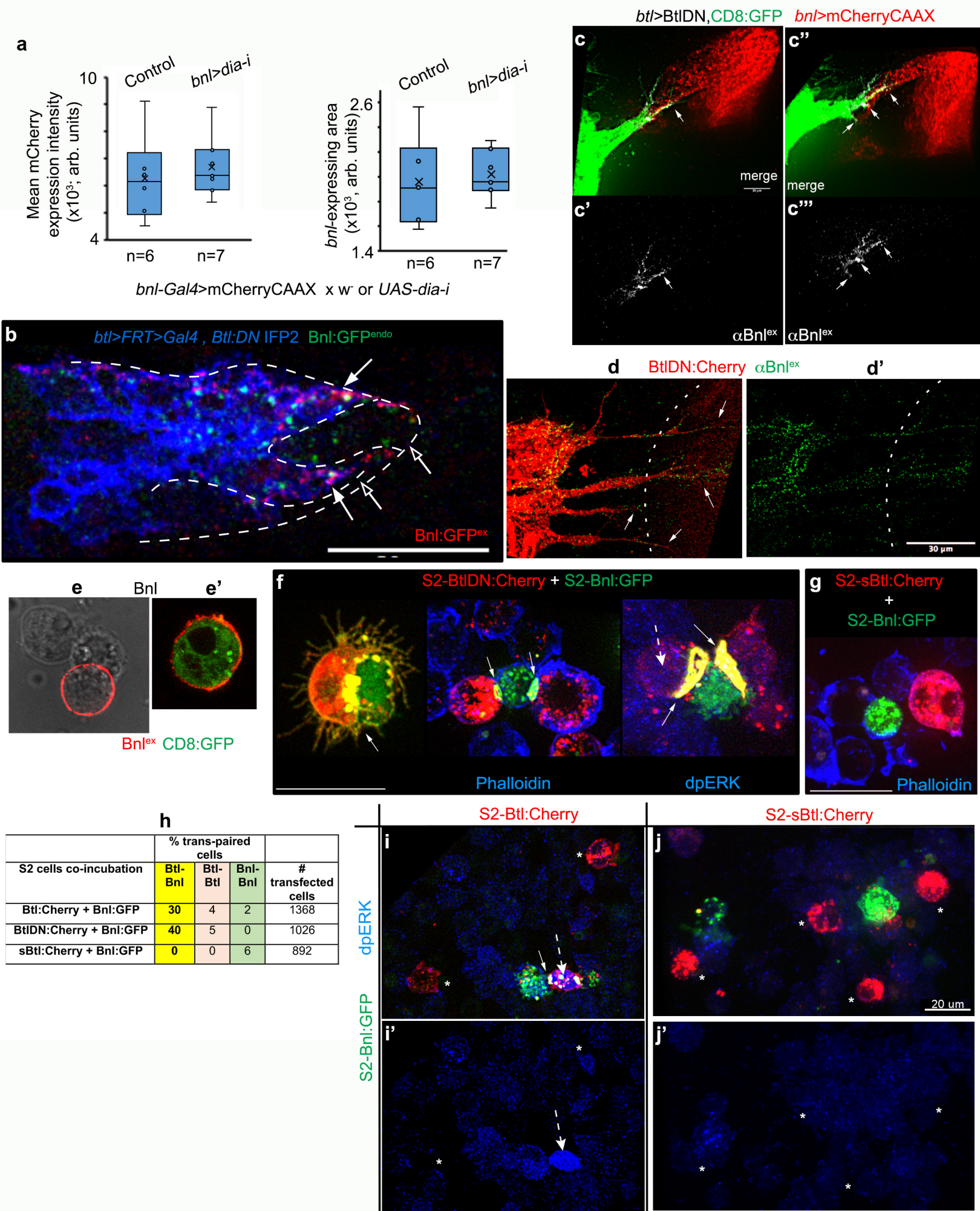
btl>CD8:GFP *bnl>CherryCAAX*



Supplementary Figure 1. Bnl sending and receiving cytonemes reciprocally guide each other.

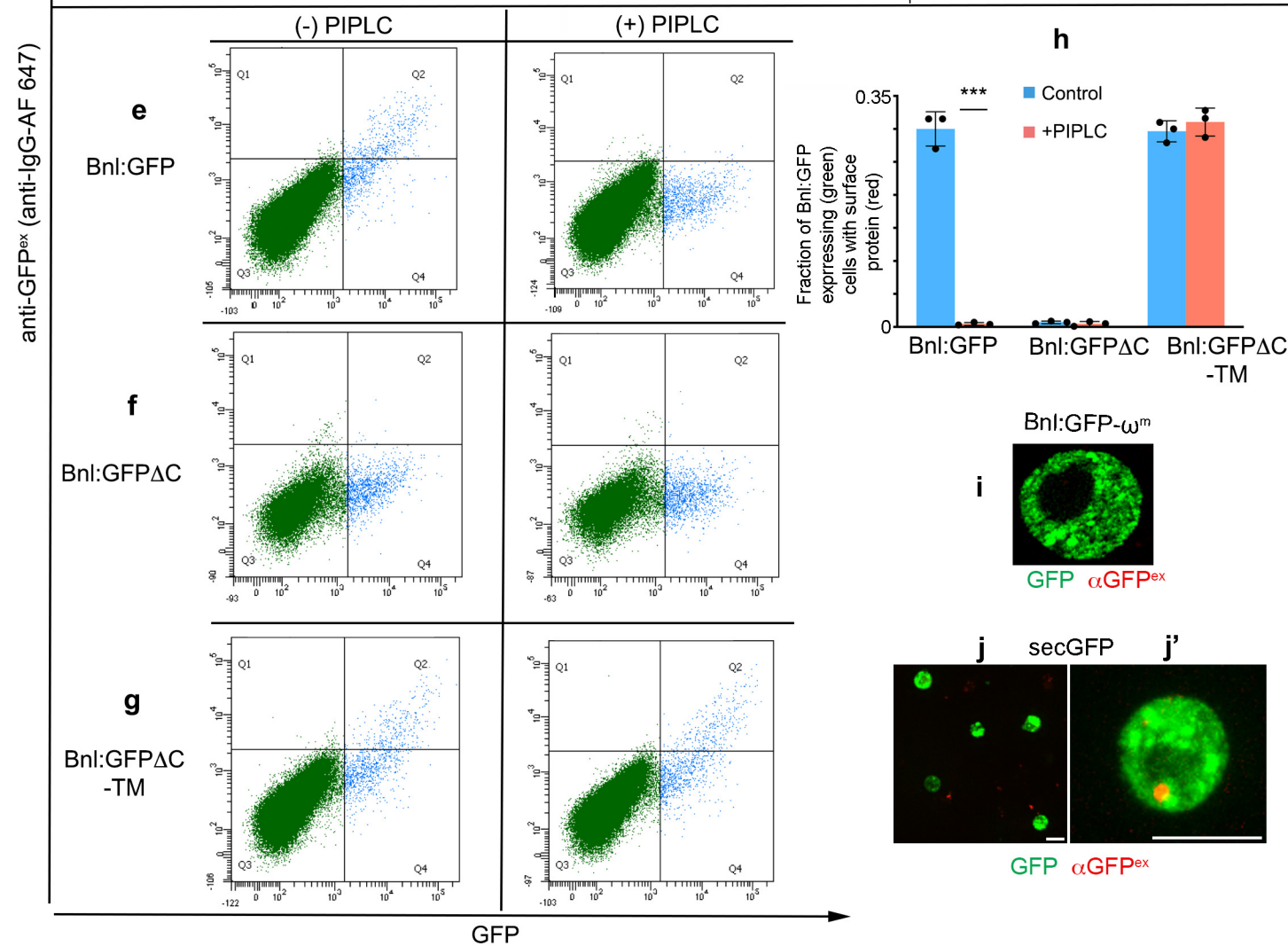
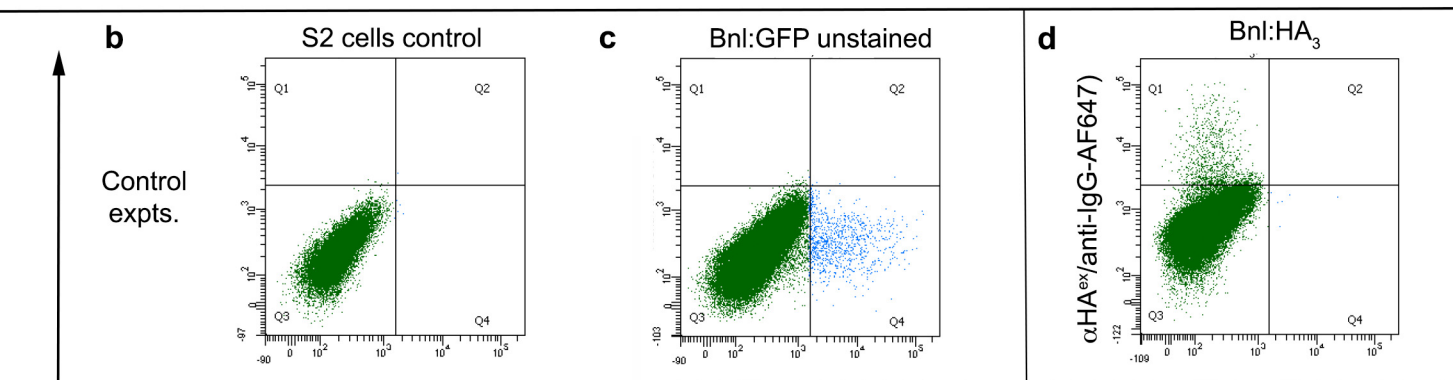
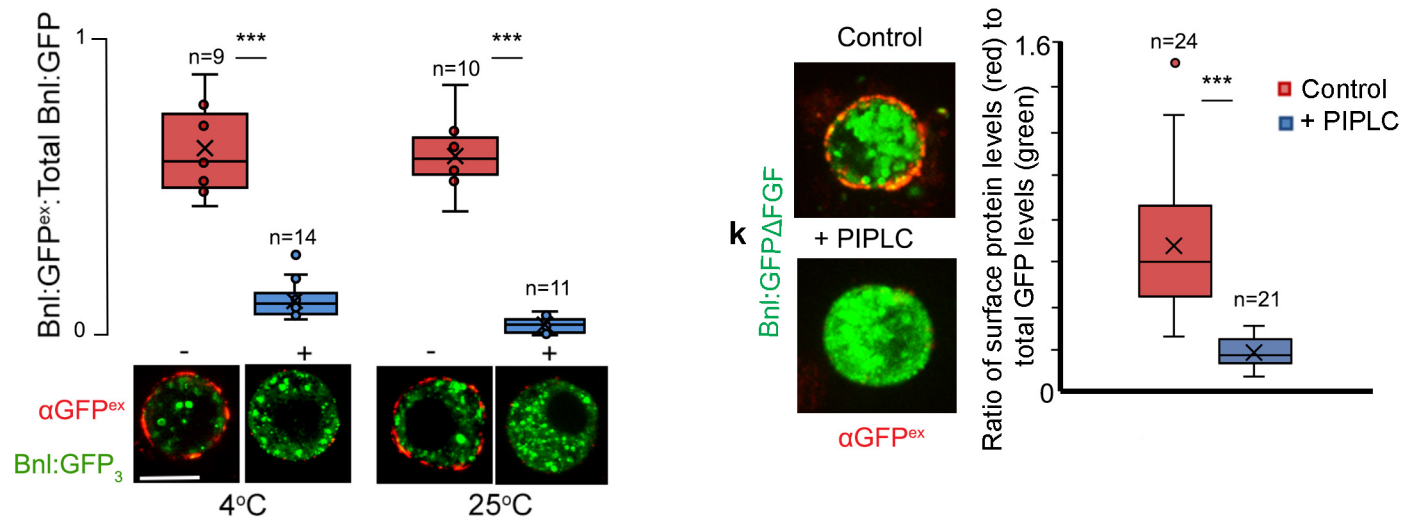
a-b Live images of mCherryCAAX-marked wing disc *bnl* source (red) expressing either Bnl:GFP by *bnl-Gal4* (a,a'; *UAS-mCherryCAAX; bnl-Gal4 X UAS-Bnl:GFP*) or endogenous Bnl:GFP^{endo} (b; *bnl:gfp^{endo}/bnl>mCherryCAAX*; spinning disc confocal), showing ASP (dashed line)-specific polarity of Bnl:GFP presentation through cytonemes (arrows). **c** A comparison of cytoneme numbers (average \pm S.D.) from the ASP and wing disc source under live and fixed imaging conditions, showing that the source cytonemes are detected mostly in live imaging. **d** Table showing the number of source cytonemes emanating from CD8:GFP-marked clones within the *bnl*-source (see Methods and Fig. 1h-h"). **e-h** Time-lapse images, showing repeated cycles of extension and retraction of source (red) and recipient (green) cytonemes for reciprocal contacts; g,h, Line plots showing interacting source and recipient cytoneme dynamics (also see Supplementary Table 1); the same color in g and h represents a pair of interacting source and ASP cytonemes. **i-l**" Maintenance of a convergently polarized cytoneme-forming niche at the ASP:source interface throughout the larval development. **e-l**" genotype - *btl-Gal4,UAS-CD8:GFP/+; bnl-LexA,lexO-mCherryCAAX/+*. Scale bars, 20 μ m. Source data are provided as a Source Data file.

Supplementary Figure 2



Supplementary Figure 2. CAM-like Btl-Bnl binding mediates reciprocal contact formation.

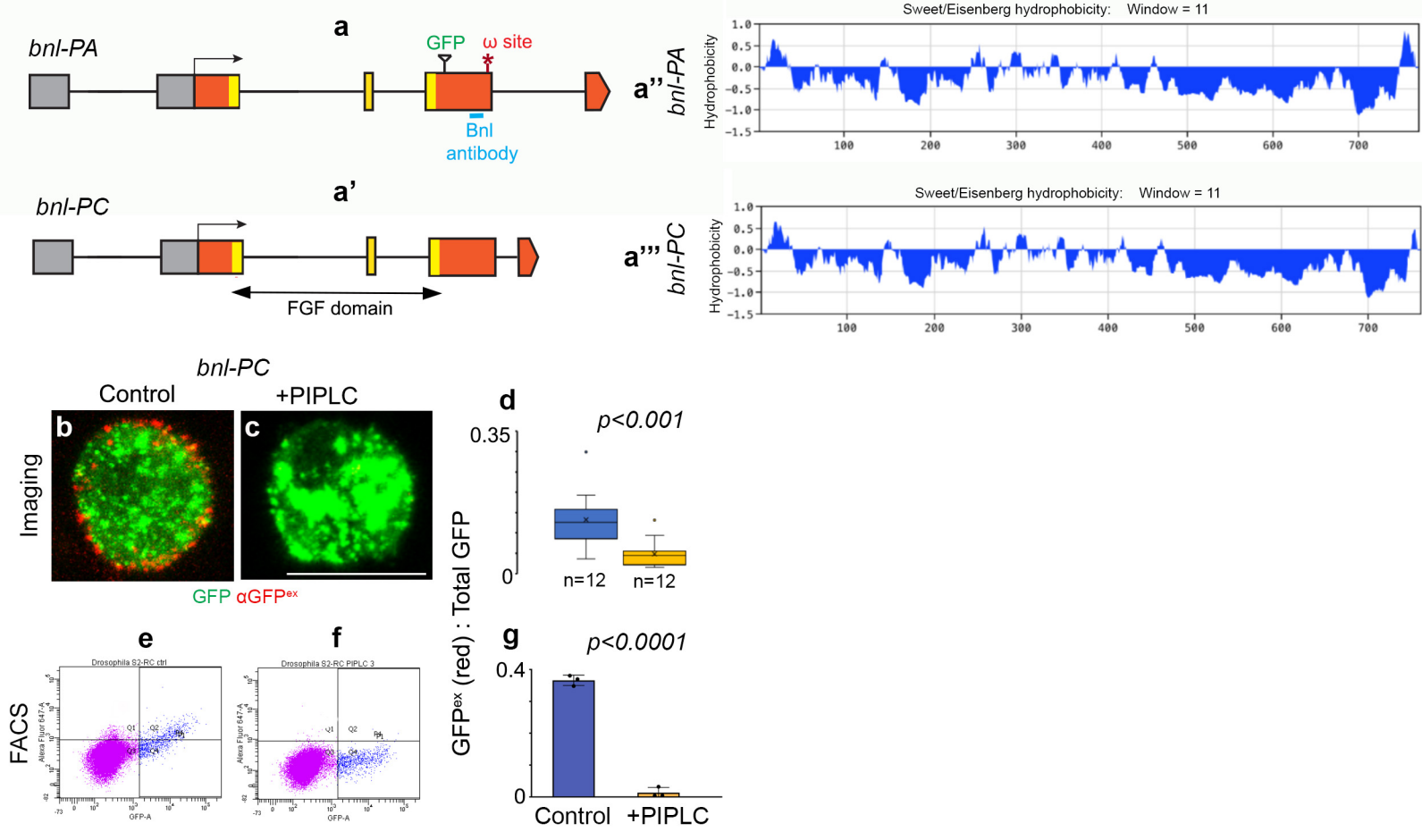
a *dia-i* expression under the *bnl-Gal4* control did not change *bnl* expression area or levels as detected by the mCherryCAAX expression (*bnl-Gal4, UAS-mCherryCAAX x UAS-dia-i* (for control, *w-* was crossed to *bnl-Gal4, UAS-mCherryCAAX*); in box plots, box shows the median as well as 1st quartile and 3rd quartile, and whiskers are minimum and maximum; n - biologically independent sample number; p values - unpaired two-tailed t-test; p=0.59 for mean mCherry expression intensity and p=0.72 for *bnl*-expressing area. **b** A mosaic ASP with Btl:DN-expressing IFP2-marked clones in the *bnl:GFP^{endo}* knock-in background (see Methods); Btl:DN-expressing surface areas on the ASP showed increased Bnl:GFP^{endo} reception from the wing disc (arrow; probed by α GFP^{ex}) compared to the WT areas (unmarked) of the same ASP tip (open arrow). **c-c'** Bnl^{ex} (grey, α Bnl^{ex}) is asymmetrically enriched (arrow) at the contact sites between source and Btl:DN-expressing ASP projections or cytonemes; c"/c'", 3D projection of c/c'. **d,d'** Btl-DN:Cherry-containing cytonemes (arrow) emanating from a rudimentary ASP localized Bnl^{ex} (green, α Bnl^{ex}) puncta on their surfaces; dashed line, source area. **e,e'** α Bnl^{ex}-stained S2 cells expressing either Bnl (e) or Bnl and CD8:GFP (e'; *act-Gal4, UAS-Bnl, UAS-CD8:GFP*), showing surface localized Bnl^{ex}, exclusively on the producing cell. **f** Different trans-paired forms of S2-Bnl:GFP and S2-Btl:DN:Cherry; arrow, trans-synaptic receptor-ligand co-clusters; dashed arrow, absence of nuclear dpERK in trans-paired S2-Btl:DN:Cherry. **g** Absence of trans-pairing between S2-sBtl:Cherry and S2-Bnl:GFP. **h** Relatively high frequency of heterotypic Btl-Bnl trans-pairing in comparison to homotypic Btl-Btl or Bnl-Bnl trans-pairing in S2-Btl:Cherry variants/S2-Bnl:GFP co-incubation assays. **i-j'** Representative examples of α dpERK-stained (blue) image frames, comparing trans-pairing experiments between S2-Bnl:GFP/S2-Btl:Cherry (i,i') and S2-Bnl:GFP/S2-sBtl:Cherry (j,j'); arrow, trans-synaptic Btl-Bnl co-cluster; dashed arrow, nucleus in trans-adhered Btl-expressing cells; *, receptor-expressing cells lacking dpERK. Scale bars, 20 μ m, 30 μ m (b,d,d'). Source data are provided as a Source Data file.



Supplementary Figure 3. A GPI anchor tethers Bnl to the source cell surface.

a-h S2 cells co-transfected with *actin-Gal4* and *UAS-X*; (X = Bnl:HA₃, Bnl:GFP₃, BnlHA₁:GFP₃ (Bnl:GFP), Bnl:HA₁:GFP₃ΔC (Bnl:GFPΔC), or Bnl:HA₁:GFP₃ΔC-TM (Bnl:GFPΔC-TM) as indicated; cells were surface immune-stained either with HA or GFP antibodies as indicated. **a**, Box plots depicting the ratio of surface localized Bnl:GFP₃ (red, αGFP^{ex} immunostaining) to total Bnl:GFP₃ (green) in S2 cells before (-) after (+) the PIPLC treatment at various temperatures; lower panels, representative images of S2 cells as indicated; box shows the median as well as 1st quartile and 3rd quartile, and whiskers are minimum and maximum; n represents # cells examined; p values were calculated using unpaired two-tailed t-test; ***, p<0.001. **b-g** Representative flow cytometry profiles of S2 cells (b, control) or S2 cells expressing various constructs as indicated; b,c,d, FACS control; d, surface αHA^{ex} staining for Bnl:HA₃ as a control profile for GFP-positive cells. **h** Bar graphs comparing mean values (± SD) obtained by flow cytometry analyses of cells from three independent transfection experiments similar to e, f, g; ***, p<0.001 (unpaired two-tailed t-test); total number of GFP+ cells: 3670 (Bnl:GFP, control), 3095 (Bnl:GFP, +PIPLC), 3240 (Bnl:GFPΔC, control), 3044 (Bnl:GFPΔC, +PIPLC), 3000 (Bnl:GFPΔC-TM, control), 3000 (Bnl:GFPΔC-TM, +PIPLC). **i** Lack of surface-localized protein (red, probed with αGFP^{ex}) of Bnl:GFP-ω^m expressed in S2 cells. **j,j'** αGFP^{ex} immunostained S2 cells expressing secGFP construct showing the lack of surface distribution of the proteins due to its immediate secretion¹. This is a control for bGFP-GPI, which is the same secGFP with Bnl's C-terminal signal sequence, leading to its GPI-anchoring to the producing cell surface (see Figure 4d'-f). **k** αGFP^{ex} immunostained S2 cells (left panels) expressing Bnl:GFPΔFGF construct showing PIPLC-sensitive surface distribution of the protein; right panel, box plots comparing the fraction of expressed protein on cell surface with and without PIPLC treatment; box shows the median as well as 1st quartile and 3rd quartile, and whiskers are minimum and maximum; n = number of cells as indicated; ***, p<0.001; p values were calculated using unpaired two-tailed t-test. Scale bars, 10 μm. Source data are provided as a Source Data file.

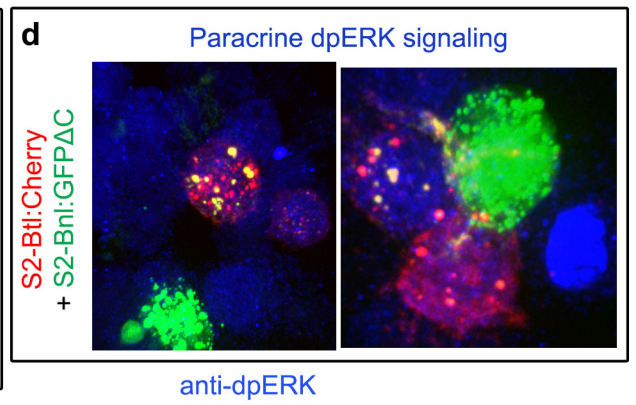
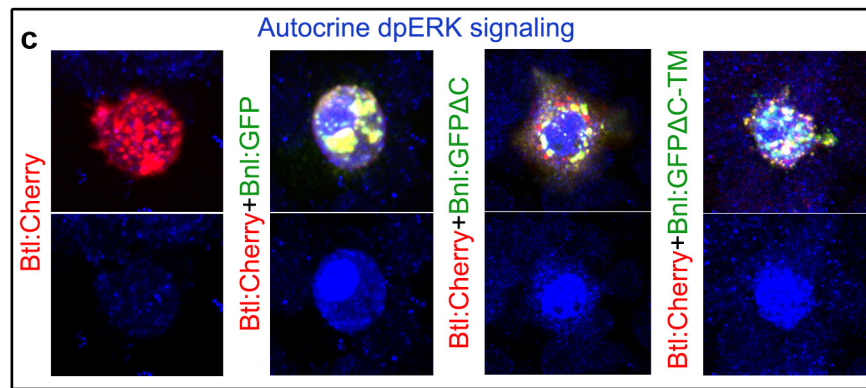
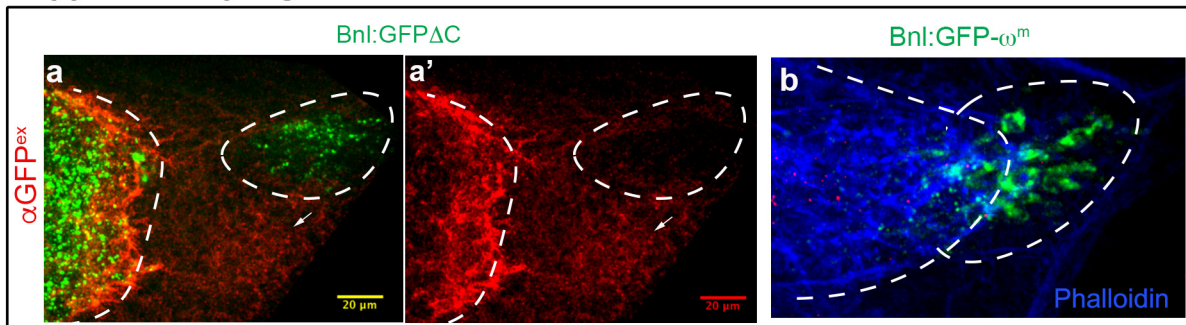
Supplementary Figure 4



Supplementary Figure 4. Characterization of GPI-anchored Bnl-PC isoform.

a-a''' Comparison of PA and PC splice variants of *bnl*: **a,a'** Schematic maps of PA and PC loci highlighting identical FGF signaling domain, Bnl antibody binding site used for probing Bnl^{ex}, GFP tag (for probing Bnl:GFP^{endo}), putative ω -site; Grey box, non-coding exons, colored box, coding exons. However, due to the alternative splicing of the last coding exons, *bnl-PC* isoform is 11 amino acid shorter at its C-terminal end than the *bnl-PA*. Subsequent to the common sequence between PA and PC, PC isoform has only 7 amino acids at its C-terminus, which is replaced by 18 amino acids sequences in PA. **a'',a'''** Comparative hydrophobicity plots of PA and PC variants showing a reduced hydrophobic stretch of C-terminal region of PC. **b-g** Extracellular α GFP^{ex}-immunostaining of S2 cells expressing Bnl:GFP₃-PC showed surface-localized Bnl:GFP₃-PC^{ex} (red), which is removed by PIPLC assay; **d** box plots showing surface localized fractions (red, probed with α GFP^{ex}) of total Bnl:GFP₃-PC expressed in S2 cells before and after PIPLC treatment; box shows the median as well as 1st quartile and 3rd quartile, and whiskers are minimum and maximum; n represents # cells examined by imaging as shown in b,c; p value was calculated using unpaired two-tailed t-test; p=0.000649. **e,f** flow cytometric analyses of the same; **g** bar graphs showing quantitative values obtained from flow cytometry experiments depicting the average fraction of Bnl:GFP₃-PC-expressing cells (GFP positive) containing surface localized Bnl:GFP₃-PC^{ex} (α GFP^{ex} immunostained (red)) before and after the PIPLC treatment; values represent the mean \pm SD from 3 independent experiments; p value was calculated using unpaired two-tailed t-test; total GFP+ events examined over 3 repeats: 3134 (control) and 2784 (+PIPLC);. Scale bars, 10 μ m. Source data are provided as a Source Data file.

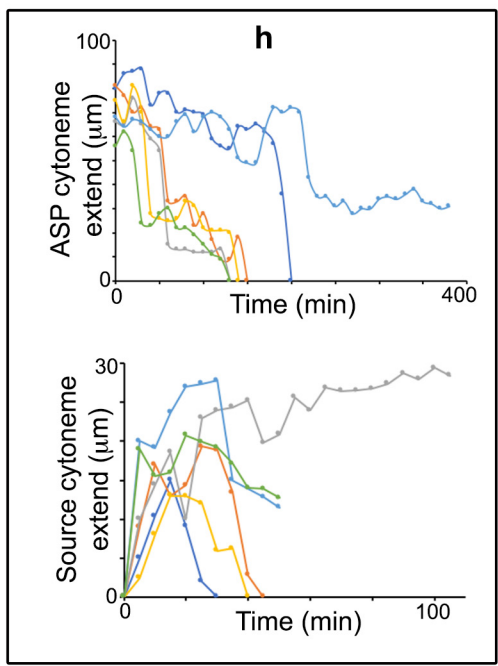
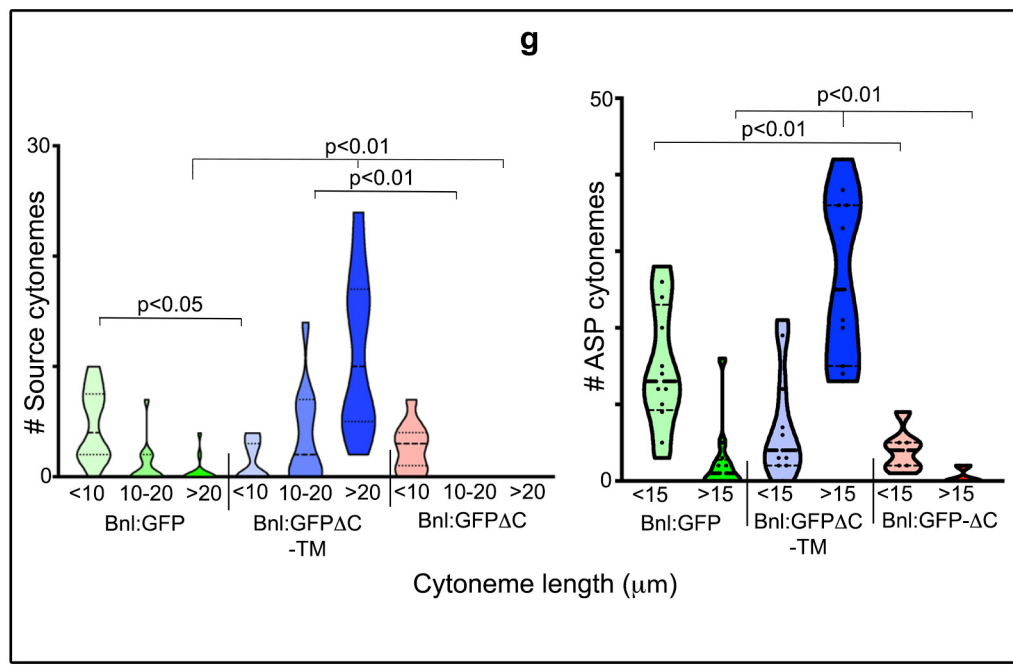
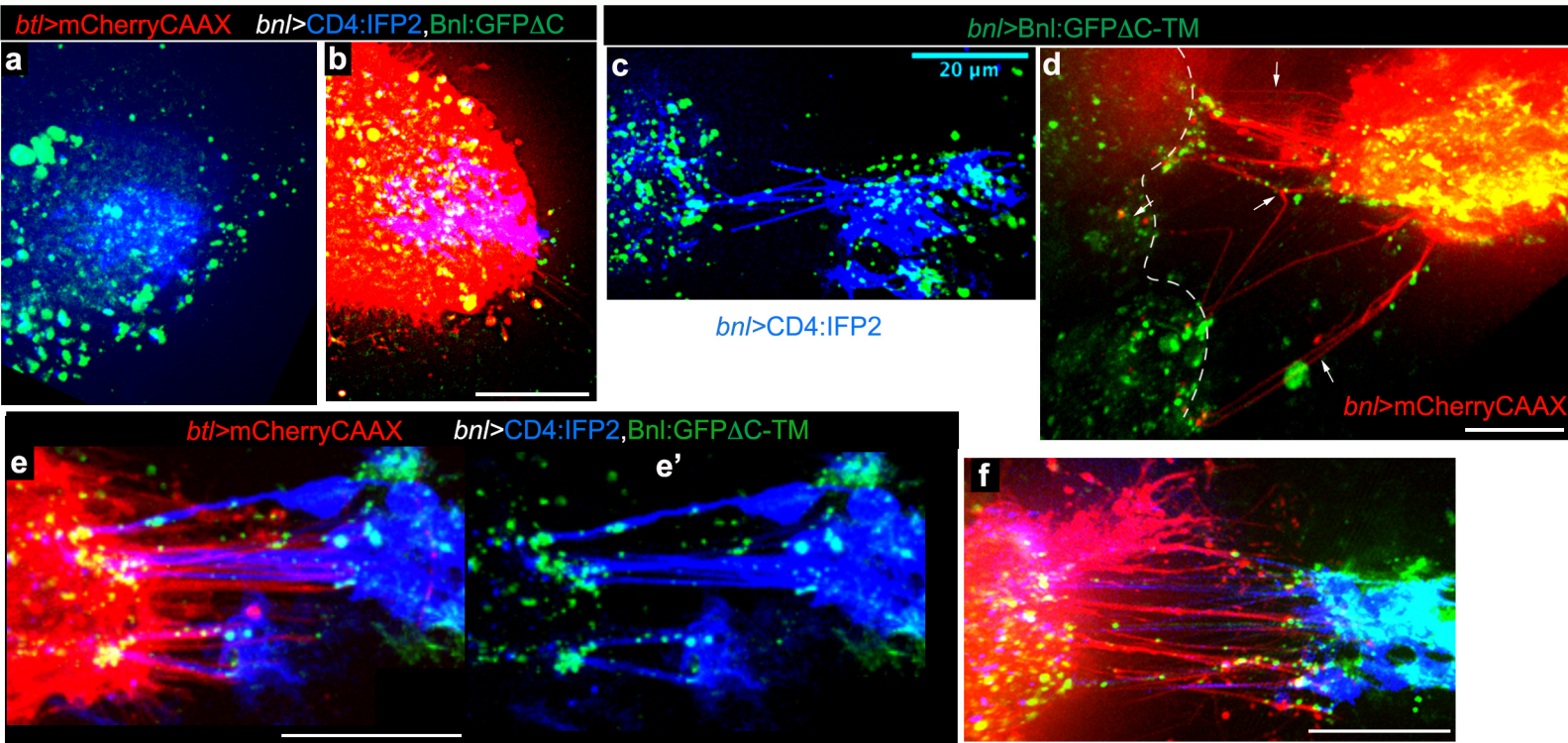
Supplementary Figure 5



Supplementary Figure 5. Autocrine and paracrine activity of Bnl variants.

a-b Extracellular distribution of Bnl:GFP Δ C (a,a') and Bnl:GFP- ω^m (b), when expressed under *bnl-Gal4* in the wing disc source; α GFP^{ex} immunostaining (red) showing that Bnl:GFP Δ C is poorly retained on the source cell surface area (green punctate demarcated by dashed line), but are spread on the extracellular plane of the non-expressing disc cells (only red). ASP had both Bnl:GFP Δ C^{ex} and internalized Bnl:GFP Δ C (probed only by GFP), showing non-autonomous signal dispersal. In contrast, Bnl:GFP- ω^m (b) is poorly externalized from the source and not received by the ASP (Phalloidin-stained). **c** Efficient autonomous MAPK signaling (nuclear dpERK, blue) of different Bnl:GFP variants when co-expressed with Btl:Cherry in S2 cells. **d** Inefficient non-autonomous MAPK signaling of Bnl:GFP Δ C when S2-Bnl:GFP Δ C cells were co-incubated with S2-Btl:Cherry cells.

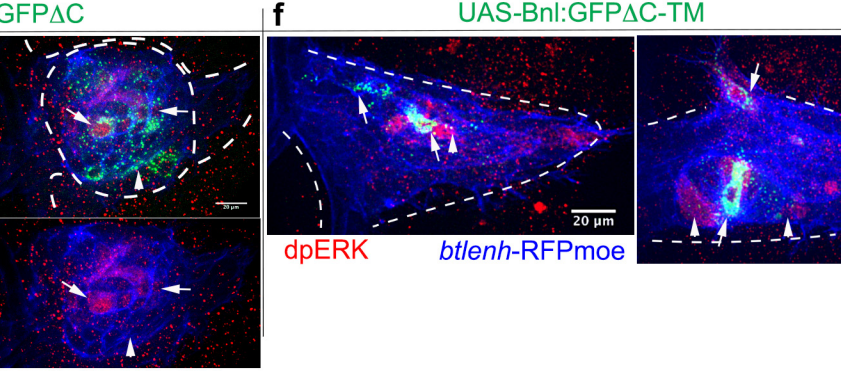
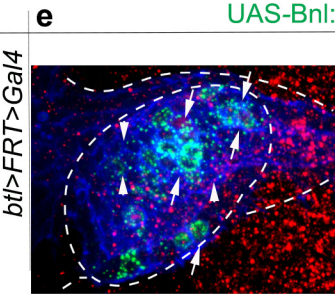
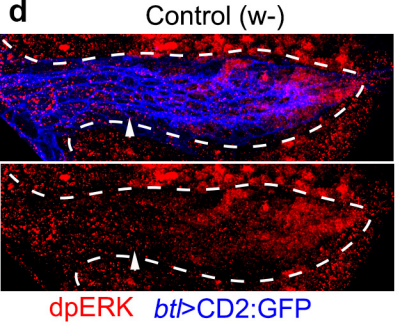
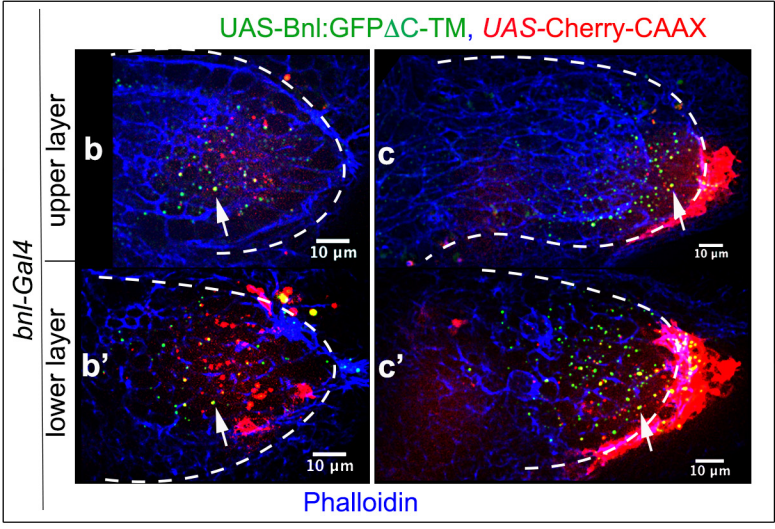
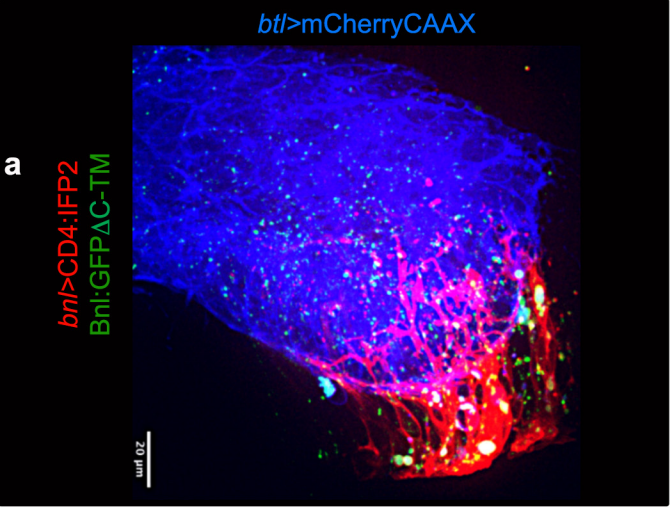
Supplementary Figure 6



Supplementary Figure 6. GPI-anchored Bnl induces cytoneme-mediated bidirectional matchmaking for contacts.

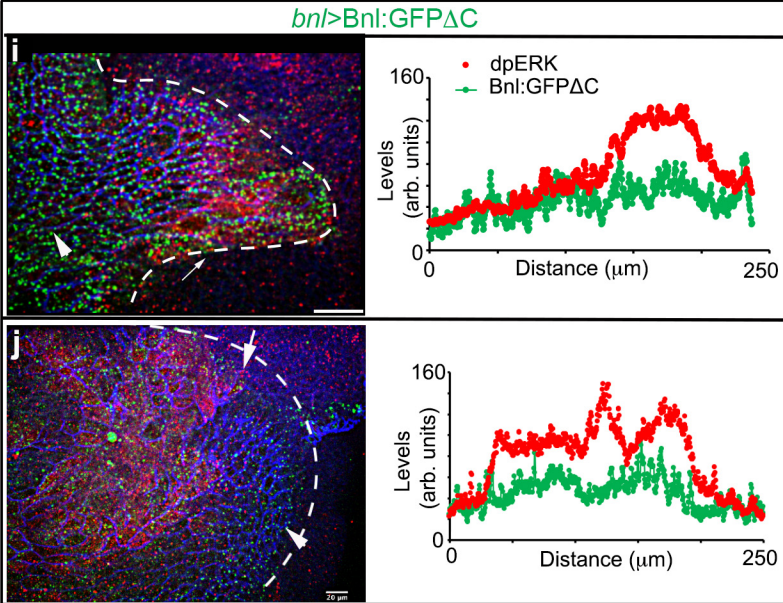
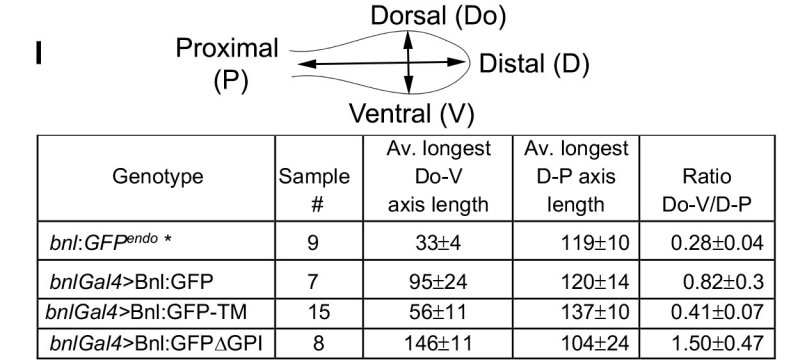
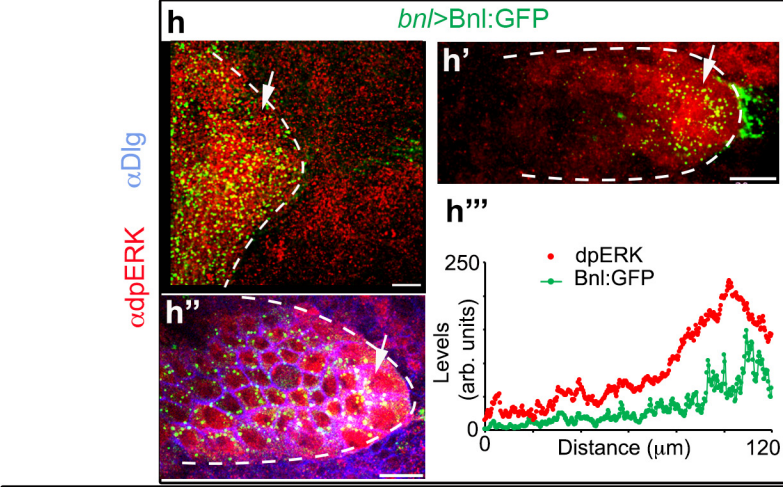
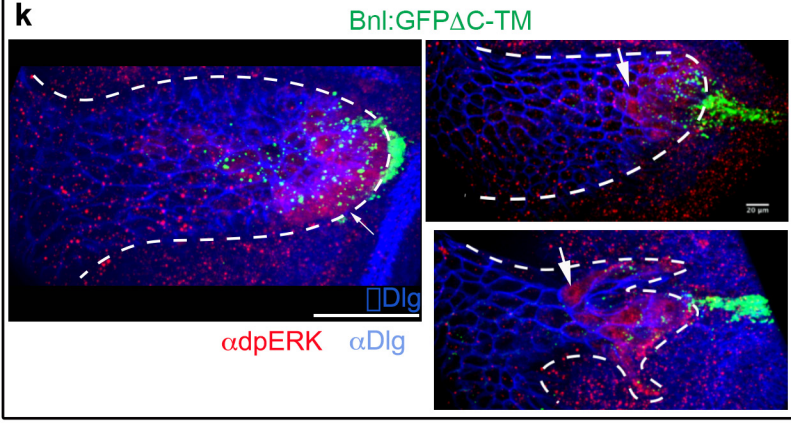
a Split channels of Figure 6g, showing the random spread of Bnl:GFP Δ C from its source (blue, *bnl>CD4:IFP2*). **b** An example showing the loss of ASP cytonemes (red), when Bnl:GFP Δ C was overexpressed from CD4:IFP2-marked source cells (blue). **c** Split green and blue channels of Figure 6j showing Bnl:GFP Δ C-TM-containing source cytonemes contacting the ASP. **d-f** Examples showing CAM-like activity of Bnl:GFP Δ C-TM when expressed from the source: (d) Long polarized Bnl:GFP Δ C-TM-expressing source cytonemes (arrows) (red, *bnl>mCherryCAAX*) connected to the ASP and disc-associated transverse connective (dashed outline). (e-f) Bundles of ASP and source cytonemes interacting through Bnl:GFP Δ C-TM-enriched lateral contact sites; e', split blue and green channels of (e). **g** Violin plots showing a comparison of the number and length distribution of ASP and source cytonemes (from Fig. 6f-l) induced by Bnl:GFP, Bnl:GFP Δ C, or Bnl:GFP Δ C-TM, when overexpressed from the disc source; in violin plots, black dotted lines show the median as well as 25th and 75th percentiles; n=13 (Bnl:GFP, source), 11 (TM, source), 11 (Δ C, source), 12 (Bnl:GFP, ASP), 11 (TM, ASP), 7 (Δ C, ASP) biologically independent samples; p values were calculated using one way-ANOVA followed by Tukey's honestly significant different test. **h** Line plots showing dynamics of the source and recipient cytonemes as indicated when Bnl:GFP Δ C-TM was expressed in *bnl* source using *bnl-Gal4* (see Supplementary Table 1); the same color represents the interacting Bnl-receiving and -sending cytonemes from the same sample. All panels, live imaging. Scale bars, 20 μ m. Source data are provided as a Source Data file.

Supplementary Figure 7



g

Genotype	Sample #	Dispersal range (# cells)	% signal receiving ASP cells with nuclear dpERK	% clones induced growth	% clones induced branching
<i>hsflp/+; btlenh>FRT>Gal4, btlenh-RFPmoe/UAS-"X"</i>					
Bnl:GFP	24	2.8±0.7	99.2±2.3	83	25
Bnl:GFP-TM	33	2.3±0.8	82.9±19.9	76	36
Bnl:GFP-ΔGPI	21	4.2±0.9	36.9±27.4	81	0



Supplementary Figure 7. GPI anchoring is required for Bnl release and morphogen-like signaling.

a Strong affinity and adhesion of Bnl:GFP Δ C-TM-expressing source cytonemes (red, *bnl>CD4:IFP2*) with the ASP surface (blue, *btl>mCherryCAAX*). **b-c'** Images of two wing discs expressing Bnl:GFP Δ C-TM and mCherryCAAX from the *bnl* source (red), showing endocytosed Bnl:GFP Δ C-TM puncta colocalized with the source membrane in upper and lower layer cells of the tubular ASP epithelium; Phalloidin-Alexa Fluor 647 (blue) marked cell outlines. **d** Control (*w-*) ASP showing the lack of nuclear dpERK in the ASP stalk and TC region, where the GOF clones were scored (see Fig. 9a-d). **e-g** Examples of ASPs with Δ C or TM GOF clones (1-2 cell size) (arrows) and their non-autonomous signaling (arrowhead; red, dpERK). **g** Table showing non-autonomous effects of Bnl:GFP, TM, and Δ C GOF clones in the ASP stalk; sample # (n) represents the number of clones examined over >10 biologically independent samples; values represent the mean \pm SD; p values for % signal receiving ASP cells with nuclear dpERK: p <0.01, for Bnl:GFP- Δ C vs. Bnl:GFP or Bnl:GFP Δ C-TM; p <0.05, for Bnl:GFP vs. Bnl:GFP Δ C-TM; p values were calculated using one way-ANOVA followed by Tukey's honestly significant different test. **h-l** Comparative analyses of the activity of Bnl:GFP, Bnl:GFP Δ C-TM (TM), and Bnl:GFP Δ C (Δ C), expressed from wing disc source under *bnl-Gal4* (*bnl-Gal4 X UAS-X*): **(h-h''')** Wing discs expressing Bnl:GFP, showing a spatial coordination of signal distribution (green puncta), signaling patterns (dpERK, red), and ASP growth. **(i-k)** The coordination between signal distribution, signaling, and growth was uncoupled by Δ C expression and was regained with TM. However, TM distribution was restricted in range in comparison to Bnl:GFP. **(l)** Comparison of ASP shapes in conditions as indicated; *, homozygous *bnl:gfp^{endo}* larvae used as the control for overexpressed Bnl:GFP variants; top panel, illustration showing the measurement of the longest Do-V and D-P axes (μ m) from extended Z-projected ASP images; sample # (n) represents the number of biologically independent samples; values represent the mean \pm SD; p values: Do-V/D-P axes: p <0.01, *bnl:gfp^{endo}* vs. Bnl:GFP or Δ C and Bnl:GFP vs. TM or Δ C; p values were calculated using one way-ANOVA followed by Tukey's honestly significant different test. h-k, arrows, recipient cells with signaling; arrowhead, recipient cells without signaling; α Dlg (blue), cell outlines. All panels, dashed line shows ASP outline or ectopic tracheal outgrowth. Scale bars, 20 μ m; 10 μ m (b-c'). Source data are provided as a Source Data file.

Supplementary Tables

Supplementary Table 1. Quantification of the dynamics of the interacting cytonemes from Bnl-receiving and -sending cells.

	FGF-receiving cells			FGF-sending cells		
	WT	<i>bnl>Bnl:GFP</i>	<i>bnl>Bnl:GFP ΔC-TM</i>	WT	<i>bnl>Bnl:GFP</i>	<i>bnl>Bnl:GFP ΔC-TM</i>
Lifetime (min)	19.55 ±6.1	17.5±5*	180±101.39	7.73± 4.67	ND	46.67±30.11
# Fluctuating peaks/lifetime	1±0	1±0	4.33±2.66	1±0	ND	2.33±1.37
Maximum extension (μm)	19.36 ±7.4	15.8±3.8	76.67±8.98	8.35±4.04	ND	26.52±7.3
Average extension rate (μm/min)	1.28 ±0.79	0.85±0.32	0.47±0.15	1.13±0.57	ND	0.70±0.23
Average retraction rate (μm/min)	1.37 ±0.75	0.93±0.19	0.88±0.22	1.32±0.56	ND	0.79±0.26

Note: Maximum extension - the maximum length of a cytoneme during its lifetime. Peak - Each extension and retraction cycle within the lifetime of a cytoneme. Number of fluctuating peaks/lifetime - the number of extension and retraction cycles of a cytoneme. Average extension and retraction rates - measured by the net cytoneme length change/time during its extension or retraction.

*, For this condition, 4 long cytonemes were used. Most cytonemes (N=25) were short in length and had lifetime <10 min and was not counted in 10 min interval time-lapse movies.

Values represent mean ± SD. N=11 cytonemes for WT; 6 cytonemes for *bnl>Bnl:GFPΔC-TM* receiving and sending cytonemes; 4 cytonemes for *bnl>Bnl:GFP* receiving cytonemes. p values (WT vs *bnl>Bnl:GFPΔC-TM*) for receiving cytoneme dynamics: lifetime, p <0.0001; # fluctuating peaks/lifetime, p <0.001; maximum extension, p <0.0001; average extension rate, p =0.025; average retraction rate, no significant difference. p values for sending cytoneme dynamics: lifetime, p <0.001; # fluctuating peaks/lifetime, p =0.0046; maximum extension, p <0.001; average extension rate, no significant difference; average retraction rate, p =0.047. p values were calculated using unpaired two-tailed t test. p < 0.05 is considered significant. Source data are provided as a Source Data file.

Genotypes: WT: *btlGal4,UAS-CD8:GFP/+;bnlLexA,LexO-mCherryCAAX/+*.

bnl>Bnl:GFP: *btlLexA,LexO-mCherryCAAX/UAS-CD4:mIFP; bnlGal4/UAS-Bnl:GFP*.

bnl>Bnl:GFPΔC-TM: *UAS-Bnl:GFPΔC-TM/UAS-CD4:mIFP; bnlGal4/btlLexA,LexO-mCherryCAAX* for FGF-receiving cytonemes, and *UAS-mCherryCAAX/UAS-Bnl:GFPΔC-TM; bnlGal4/+* for FGF-sending cytonemes.

Supplementary Table 2. Comparison of the ASP and source cytoneme numbers when *diaRNAi* was expressed in the ASP.

		# ASP cytonemes < 15 μ m	# ASP cytonemes > 15 μ m	# FGF source cytonemes
Control (N=11)	Average	11.55	17	9.45
	SD	\pm 4.57	\pm 4.96	\pm 3.30
<i>btlGal4>diaRNAi</i> (N=8)	Average	10	1	0
	SD	\pm 7.66	\pm 1.06	\pm 0.35
<i>p</i> (unpaired t-test)		0.559367458	5.87525E-08	4.27454E-07

Note: Values represent mean \pm SD. N represents the number of biologically independent samples. *p* values were calculated using unpaired two-tailed t test. Source data are provided as a Source Data file.

Genotypes: Control: *btlGal4,UAS-CD8GFP/+;bnlLexA,LexO-mCherryCAAX/+*.

btl-Gal4>diaRNAi: *btlGal4,UAS-CD8GFP/tub-Gal80^{ts};bnl-LexA,LexO-mCherryCAAX/ UAS-diaRNAi*.

Supplementary Table 3: Autocrine and paracrine MAPK signaling activity of Bnl:GFP variants in S2 cells

a. Autocrine activity: S2-Btl:Cherry co-expressed with Bnl:GFP variants

S2 cell co-expression	# total Btl cells	# Btl cells with nuclear dpERK	% Btl cells with nuclear dpERK
Bnl:GFP+Btl:Cherry	15	14	93
Bnl:GFP Δ GPI+Btl:Cherry	22	21	95
Bnl:GFP Δ GPI-TM +Btl:Cherry	16	15	94

b. Paracrine activity: S2-Bnl:GFP variants co-incubated with S2-Btl:Cherry

S2-Btl:Cherry cells (# or %)	Bnl:GFP +Btl:Cherry	Bnl:GFP Δ GPI +Btl:Cherry	Bnl:GFP Δ GPI-TM +Btl:Cherry
# of total cells (A)	169	188	123
# of (A) with dpERK	76	65	60
% of (A) with dpERK	44.9	34.6*	48.8
# of trans-paired cells with S2-Bnl:GFP/TM or adjacent to S2- Δ C (B)	78	33	87
# of (B) with dpERK	71	5	58
% of (B) with dpERK	91	15**	67
# of uncoupled Btl +ve cells (C)	91	188	36
# of (C) with dpERK	5	60	2
% of (C) with dpERK	5	32 **	6

Note: data represents results from three independent transfection repeats.

Supplementary Table 4: Resources and reagents used in this study

REAGENT or RESOURCE	DESCRIPTION	SOURCE
Antibodies		
Mouse monoclonal anti-Discs large (Dlg)	1:100	DSHB, Cat# 4F3 anti-discs large; RRID: AB_528203
Phospho-p44/42 MAPK (Erk1/2) (Thr202/Tyr204) rabbit monoclonal antibody (dpERK)	1:250 in tissue and 1:1000 in S2 cells	Cell signaling Technology; Cat# 4370; RRID: AB_2315112
Rat monoclonal anti-HA (3F10)	1:1000 for standard and 1:500 for EIF	Roche; Cat#1186742300 1; RRID: AB_390918
Rabbit polyclonal anti-Bnl	1:500 for EIF ¹	N/A
Rabbit anti-GFP antibody	1:3000 for EIF	Abcam; Cat# ab6556; RRID: AB_305564
Goat anti-Mouse IgG (H+L), Alexa Fluor 555	1:1000	Thermo Fisher Scientific; A21434
Goat anti-Mouse IgG (H+L), Alexa Fluor 647	1:1000	Thermo Fisher Scientific; A28181
Goat anti-Rat IgG (H+L), Alexa Fluor 647	1:1000	Thermo Fisher Scientific; A21247
Goat anti-Rabbit IgG (H+L), Alexa Fluor 555	1:1000	Thermo Fisher Scientific; A21428
Goat anti-Rabbit IgG (H+L), Alexa Fluor 647	1:1000	Thermo Fisher Scientific; A21244
Bacterial and Virus Strains		
DH5 Alpha		
Chemicals, Peptides, and Recombinant Proteins		
Alexa Fluor 647 Phalloidin	Thermo Fisher Scientific	Cat# A22287, RRID: AB_2620155
Furin Inhibitor I - Calbiochem	Sigma-Aldrich	Cat# 344930
Furin Inhibitor II - Calbiochem	Sigma-Aldrich	Cat# 344931
Phospholipase C, Phosphatidylinositol-specific from <i>Bacillus cereus</i>	Invitrogen	Cat# P6466
Critical Commercial Assays		
Lipofectamine 3000 Transfection Reagent	Thermo Fisher Scientific	Cat# L3000008
Mirus TransIT [®] -Insect Transfection Reagent	Mirus Bio	
TRI Reagent	Sigma-Aldrich	Cat# T9424
OneTaq [®] One-Step RT-PCR Kit	NEB	Cat# E5315S
Deposited Data		
Raw data from all the figures	This paper	
Experimental Models: Cell Lines		
<i>D. melanogaster</i> . Cell line S2: S2-DRSC	Laboratory of Thomas B. Kornberg	FlyBase: FBtc0000181
Experimental Models: Organisms/Strains		
<i>D. melanogaster</i> . UAS-Bnl:GFP Δ C	This paper	N/A
<i>D. melanogaster</i> . UAS-Bnl:GFP Δ C-TM	This paper	N/A

<i>D. melanogaster. UAS-Bnl:GFPΔC₁₆₈-TM</i>	This paper	N/A
<i>D. melanogaster. UAS-Bnl:GFPΔC₁₆₈</i>	This paper	N/A
<i>D. melanogaster. LexO-BtlDN:Cherry</i>	This paper	N/A
<i>D. melanogaster. UAS-Bnl:GFP-ω^m</i>	This paper	N/A
<i>D. melanogaster. bnl:gfp^{endo}</i>	1	N/A
<i>D. melanogaster. btl:cherry^{endo}</i>	1	N/A
<i>D. melanogaster. UAS-Bnl:GFP</i>	2	N/A
<i>D. melanogaster. UAS-CD8:GFP</i>	BDSC	5137
<i>D. melanogaster. UAS-nlsGFP</i>	BDSC	4776
<i>D. melanogaster. UAS-mCherryCAAX</i>	BDSC	59021
<i>D. melanogaster. UAS-CD4:mIFP</i>	BDSC	64182
<i>D. melanogaster. lexO-mCherryCAAX</i>	3	N/A
<i>D. melanogaster. UAS-Btl^{DN}</i>	4	N/A
<i>D. melanogaster. UAS-Bnl</i>	BDSC	64232
<i>D. melanogaster. UAS-diaRNAi</i>	BDSC	33424
<i>D. melanogaster. UAS-Dia-GFP</i>	3	N/A
<i>D. melanogaster. UAS-ΔDAD-Dia-GFP</i>	3	N/A
<i>D. melanogaster. bnl-LexA</i>	1	N/A
<i>D. melanogaster. bnl-Gal4</i>	BDSC	112825
<i>D. melanogaster. btl-Gal4</i>	5	N/A
<i>D. melanogaster. btl-LHG</i>	3	N/A
<i>D. melanogaster. hs-FLP; btl>y+>Gal4, btl-mRFP1moe</i>	6	N/A
<i>D. melanogaster. hs-mFlp</i>	BDSC	N/A
<i>D. melanogaster. FlyBow FB2.0</i>	BDSC	N/A
<i>D. melanogaster. btl:GFP fTRG</i>	VDRC	318302
<i>D. melanogaster. hs-Flp</i>	BDSC	6
<i>D. melanogaster. tub-Gal80^{ts}</i>	BDSC	7108
<i>D. melanogaster. act>CD2>Gal4</i>	BDSC	4780
<i>D. melanogaster. w¹¹¹⁸</i>	BDSC	3605
Oligonucleotides		
Primer for cloning <i>UAS-Bnl:GFPΔC</i> : GCCAAGCTTGCATGCCGGTACCTTAGTAGCTCGCATCTT CTAGGGATCC	This paper	N/A
Primer for cloning <i>UAS-Bnl:GFPΔC-TM</i> : CCCTAGAAGATGCGAGCTACGACTTCGCCTGTGATATTT ACATCTGG	This paper	N/A
Primer for cloning <i>UAS-Bnl:GFPΔC-TM</i> : GATGTAAATATCACAGGCCGAAGTCGTAGCTCGCATCTTC TAGGGATCC	This paper	N/A
Primer for cloning <i>UAS-Bnl:GFPΔC-TM</i> : GCCAAGCTTGCATGCCGGTACCTTAGTGGTAGCAGATG AGAGTGATGATC	This paper	N/A
Primer for cloning <i>UAS-Bnl:GFPΔC₁₆₈</i> : GCCAAGCTTGCATGCCATATATTCTAGATTACTTCTTCTT GCCTCCGTGCTG	This paper	N/A
Primer for cloning <i>UAS-Bnl:GFPΔC₁₆₈-TM</i> : CAGCACGGAGGCAAGAAGgacttcgctgtgatatttacatctgg	This paper	N/A
Primer for cloning <i>UAS-Bnl:GFPΔC₁₆₈-TM</i> : ccagatgtaaatatcacaggcgaagtcCTTCTTCTGCCTCCGTGCT G	This paper	N/A
Primer for cloning <i>UAS-Bnl:HA₁GFP₃Cherry_c</i> : GTTTTGCTCCGAAAAAGGCCATCTGATGGTGAGCAAG GGCGAGGAG	This paper	N/A
Primer for cloning <i>UAS-Bnl:HA₁GFP₃Cherry_c</i> : GCTGCTGGTACCTTACTTGTACAGCTCGTCCATGCCG	This paper	N/A

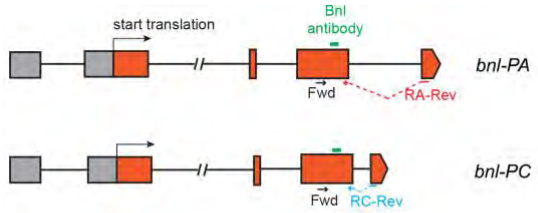
Primer for cloning <i>UAS-Bnl:GFP-ω^m</i> : CGAGGCCCAAGGACGCCCCACCAGGCGGCGACGAT TCG	This paper	N/A
Primer for cloning <i>UAS-Bnl:GFP-ω^m</i> : CGAATCGTCGCCGCTGGTGGGGGGCGTCCTTGGGCC TCG	This paper	N/A
Primer for cloning <i>UAS-bGFP-GPI</i> : CAACAACCTTGACAATGTCCAAGGGCGAGGAG	This paper	N/A
Primer for cloning <i>UAS-bGFP-GPI</i> : GCCCTTGGACATTGTCAAGTTGTTGTCCATGGCC	This paper	N/A
Primer for cloning <i>UAS-bGFP-GPI</i> : TGGATGAGCTGTACAAGACCGAGGGCGACGGTG	This paper	N/A
Primer for cloning <i>UAS-bGFP-GPI</i> : TCGGTCTTGACAGCTCATCCATGCC	This paper	N/A
Primer for cloning <i>UAS-Bnl:GFPΔFGF</i> : CCCTTGGACATGGACTGTGGCACCGTGG	This paper	N/A
Primer for cloning <i>UAS-Bnl:GFPΔFGF</i> : TGCCACAGTCCATGTCCAAGGGCGAGGAGC	This paper	N/A
Primer for cloning <i>UAS-Bnl:GFPΔFGF</i> : CACCGTCTTGACAGCTCATCCATGCC	This paper	N/A
Primer for cloning <i>UAS-Bnl:GFPΔFGF</i> : ATGAGCTGTACAAGACGGTGGCGCAGGAG	This paper	N/A
Forward primer for cloning all the constructs above: AATTCGAGCTCGGTACAGATCTATGCGAAGAAACCTGCG C	This paper	N/A
Primer for cloning <i>UAS-sBtl:Cherry</i> : AATTCGAGCTCGGTACCTCGAGATGGCAAAGTGCCGAT CACG	This paper	N/A
Primer for cloning <i>UAS-sBtl:Cherry</i> : GCCGCCTTGCCCTCGACAGGATGGGCGTGCAGCAG	This paper	N/A
Primer for cloning <i>UAS-sBtl:Cherry</i> : GTGCGAGGGGCAAGGCGGCatggtgagcaagggcgag	This paper	N/A
Primer for cloning <i>UAS-sBtl:Cherry</i> : GCCAAGCTTGCATGCCTCTAGAttactgtacagctcgccatgcc	This paper	N/A
Forward primer for <i>bnl</i> RT-PCR: CAGGAGGACACTACAATTGCCAG	This paper	N/A
Reverse primer for <i>bnl</i> -RA RT-PCR: GCTGCAGACACAGGAAATCG	This paper	N/A
Reverse primer for <i>bnl</i> -PC RT-PCR: GGGACAACAGTCCGAAATCG	This paper	N/A
Primer for cloning <i>UAS-Bnl^{PC}:GFP</i> : GCCAAGCTTGCATGCCATATATTCTAGATCATCGCCGGG GGGACAACAGTCCGAAATCGTAGTAGAGCGAATCGTCCG	This paper	N/A
Recombinant DNA		
pUAST-Bnl:GFP	2	N/A
pUAST-Bnl:HA	2	
pUAST-Bnl:HA ₁ GFP ₃ (<i>UAS</i> -HA ₁ Bnl:GFP ₃)	2	
pUAST-GFP-GPI	7	N/A
pUAST-cSpi:GFP	8	N/A
pUAST-Bnl:GFP Δ C ₄₀ (Δ C) & -Bnl:GFP Δ C ₁₆₈	<i>UAS-Bnl:HA₁GFP₃</i> by deleting the last 40 (after Y ₇₃₀ of Bnl) and 168 (after K ₆₀₂ of Bnl) amino acid regions, respectively, prior to a stop codon.	N/A
pUAST-Bnl:GFP Δ C-TM & -Bnl:GFP Δ C-TM ₁₆₈	a 31 amino acid long transmembrane domain of the mammalian CD8a protein fused to the C-terminus of <i>UAS-Bnl:GFPΔC</i> and <i>UAS-Bnl:GFPΔC₁₆₈</i> , respectively.	N/A

pUAST-Bnl:GFP ₃ Cherry _c	<i>UAS-Bnl:HA₁GFP₃</i> with a C-terminal mCherry tag with a linker (VEGQGG) placed in between.	N/A
pUAST-Bnl _{PC} :GFP	The PC-specific C-terminal 24 bp sequence (7 amino acids+stop) was added to the C-terminus of the 1-2259 bp region of <i>bnl-PA</i> CDS using PCR	N/A
pUAST-Bnl:GFP- ω^m	<i>UAS-Bnl:HA₁GFP₃</i> with mutated ω , $\omega+1$, and $\omega+2$ sites (S/P ⁷⁴¹ G/P ⁷⁴² A/P ⁷⁴³)	N/A
pUAST-bGFP-GPI	secGFP ¹ (superfolder GFP with N-terminal Bnl signal peptide) added with the last 53 amino acids of Bnl (from T ₇₁₈) at the C-terminus.	N/A
pUAST-sBtl:Cherry	mCherry sequence was added in-frame after P ⁶⁰⁷ of Btl, replacing the TM and intracellular portions.	N/A
pUAST-BtlDN:Cherry and pLot-BtlDN:Cherry	mCherry sequence was added in-frame after L ₆₂₅ of Btl, replacing the intracellular C-terminal portions.	N/A
pUAST-Bnl:GFP ^{ΔFGF}	Conserved FGF domain of Bnl was replaced with a sfGFP sequence	N//A
Software and Algorithms		
Fiji	ImageJ	https://fiji.sc
Prism 8.0	GraphPad	https://www.graphpad.com/
Adobe Photoshop	Adobe	https://www.adobe.com
Adobe Illustrator	Adobe	https://www.adobe.com
Microsoft Excel	Microsoft	https://www.office.com
SnapGene	SnapGene	https://www.snapgene.com
MacVector	MacVector	https://macvector.com
PredGPI predictor		http://gpcr.biocomp.unibo.it/predgpi/pred.htm
VassarStats		vassarstats.net
R x64 3.3.1	R	r-project.org
Imaris 9.5.0	Imaris	https://imaris.oxinst.com

Supplementary Notes

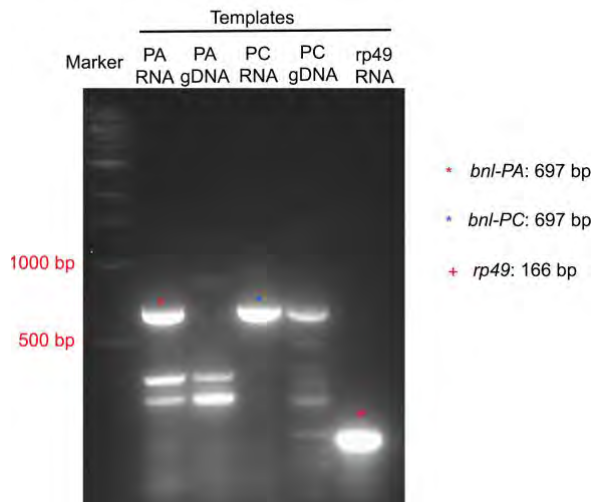
A. Expression analyses of *bnl* splice variants using RT-PCR

The *bnl* gene has two different splice variants encoding proteins with different C-terminal



hydrophobic sequences. To check the expression of different *bnl* isoforms, total RNA was extracted from 20 *w¹¹¹⁸* larval wing discs and RT-PCR was performed on the total RNA. For both isoforms, we used a common forward primer that binds to exon 3 (5'-CAGGAGGACACTCACAATTGCCAG-3').

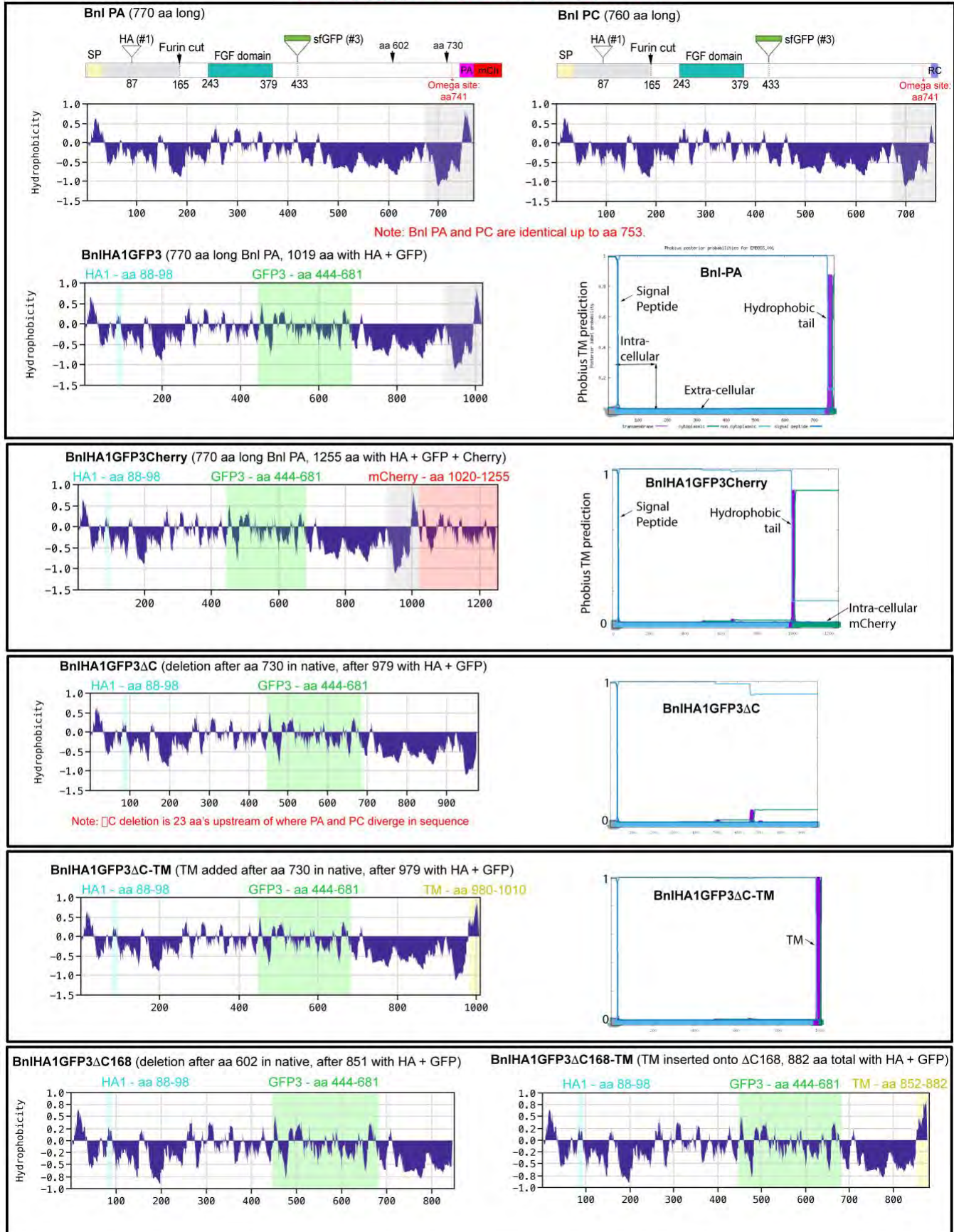
However, the reverse primers were either PA- (5'-GCTGCAGACACAGGAAATCG-3') and PC- (5'-GGGACAACAGTCCGAAATCG-3') -specific. The reverse primer for each isoform was designed to span the junction between exon 3 and the isoform-specific last exon as illustrated below. The expected amplicon size was 697bp. As a negative control, RT-PCR was carried out on the genomic DNA (gDNA)



template obtained from *w¹¹¹⁸* flies. As a positive control we performed RT-PCR for constitutive *rp49* gene. Unsurprisingly, RT-PCR results showed strong amplification of *bnl-PA*, exclusively from the RNA template. Although we detected strong *bnl-PC* amplification from the RNA template, we also detected a low level amplification of the same sized RT-PCR product from gDNA. These results confirmed *bnl-PA* expression in the wing disc. These results, although not conclusive, also suggested that the wing disc expresses *bnl-PC*. Moreover, a Bnl antibody, which detects both isoforms, showed that the native Bnl^{ex} is asymmetrically localized on the wing disc producing cell surface and the Bnl^{ex} was reduced with the PIPLC treatment. Secondly, S2 cells expressing a chimeric Bnl^{PC}:GFP construct showed the PIPLC-sensitive surface distribution of the protein. Based on these results, we suggest that irrespective of the tissue-specific expression levels, Bnl isoforms are GPI-anchored on the cell surface. Consistent RT-PCR results were obtained from three independent experiments, confirming the expression profile.

B. Bioinformatic analyses of hydropathy and secondary topology of various Bnl constructs

Note: hydropobicity plots - Sweet/Eisenberg hydropobicity: Window = 11



C. Comparison of *bnl-GAL4*-driven expression levels of transgenic constructs

Transgenic Constructs	Fly line	Chromosomal Insertion	Expression levels *	externalized by source?	ASP uptake?
UAS-Bnl:GFP Δ C ₄₀	2_2	3	+++	Yes	Yes
	3_1	3	ND	n/a	n/a
	3_2	2	++	Yes	Yes
UAS-Bnl:GFP Δ C ₄₀ -TM	1_2	3	+++	Yes	Yes (R)
	2_2	2	+++	Yes	Yes (R)
	3_1	3	++	Yes	Yes (R)
	3_2	2	++	Yes	Yes (R)
	4_1	2	++	Yes	Yes (R)
	6_1	3	ND	n/a	n/a
	7_1	3	+	Yes	Yes (R)
	9_2	3	+++	Yes	Yes (R)
UAS-Bnl:GFP Δ C ₁₆₈	1_2	2	++	Yes	Yes
	4_1	3	+++	Yes	Yes
UAS-Bnl:GFP Δ C ₁₆₈ -TM	1_1	3	++	Yes	Yes (R)
	2_1	3	+++	Yes	Yes (R)
UAS-Bnl:GFP- ω^m	1_1	3	+++	L	L
	4_1	2	+++	L	L

* Expression levels were verified by *bnl-Gal4* driven expression of the *UAS* constructs in the wing disc *bnl* source (see Methods). Bnl:GFP lines used in this study was published earlier in Du et al. and Sohr et al.^{1,2}. ND: Not detected. Red: Lines with comparable expression levels used in this study. R: Restricted range. L: Very low level.

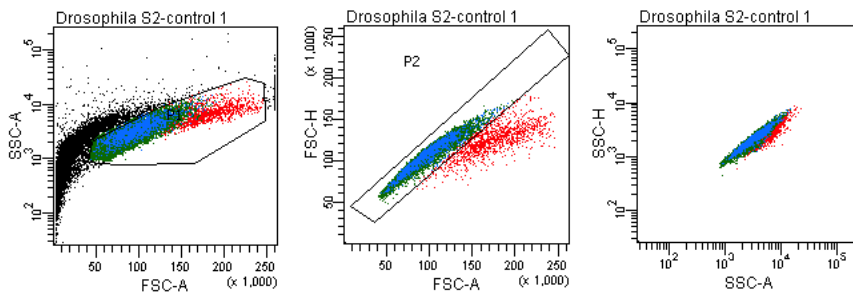
+++ > ++ > + : High > medium > low levels of expression relative to each other.

An example of comparison of levels of expression of Bnl:GFP variants under *bnl-Gal4* in the wing disc

	Bnl:GFP	Bnl:GFP Δ C ₄₀ (2_2)	Bnl:GFP Δ C ₄₀ -TM (2_2)
Mean GFP intensity in the <i>bnl</i> -source (derived from extended Z-stack of 50 μ m tissue)	1137.40	867.5	1495.3
	1142.2	1106.3	899.7
	1870.1	2400.1	620.6
	747.7	909.8	1372.5
(7 wing discs from 7 animals used)	1190.05	782.9	610.1
	972.8	985.5	1868.6
	527.6	484.3	1126.298
Average	1083.98*	1076.63*	1141.87*

*, Comparable levels of expression of different constructs used in this study.

D. Examples of gating strategy for FACS analyses



Supplementary References

1. Du, L., Sohr, A., Yan, G. & Roy, S. Feedback regulation of cytoneme-mediated transport shapes a tissue-specific FGF morphogen gradient. (2018).
2. Sohr, A., Du, L., Wang, R., Lin, L. & Roy, S. Drosophila FGF cleavage is required for efficient intracellular sorting and intercellular dispersal. *J Cell Biol* 218, 1653–1669 (2019).
3. Roy, S., Huang, H., Liu, S. & Kornberg, T. B. Cytoneme-mediated contact-dependent transport of the Drosophila decapentaplegic signaling protein. *Science (New York, N.Y.)* 343, 1244624 (2014).
4. Reichman-Fried, M. & Shilo, B.-Z. Breathless, a Drosophila FGF receptor homolog, is required for the onset of tracheal cell migration and tracheole formation. *Mech Develop* 52, 265–273 (1995).
5. Sato, M. & Kornberg, T. B. FGF Is an Essential Mitogen and Chemoattractant for the Air Sacs of the Drosophila Tracheal System. *Dev Cell* 3, 195–207 (2002).
6. Cabernard, C. & Affolter, M. Distinct Roles for Two Receptor Tyrosine Kinases in Epithelial Branching Morphogenesis in Drosophila. *Dev Cell* 9, 831–842 (2005).
7. Greco, V., Hannus, M. & Eaton, S. Argosomes: a potential vehicle for the spread of morphogens through epithelia. *Cell* 106, 633–645 (2001).
8. Miura, G. I. *et al.* Palmitoylation of the EGFR ligand Spitz by Rasp increases Spitz activity by restricting its diffusion. *Developmental Cell* 10, 167–176 (2006).
9. Greco, V., Hannus, M. & Eaton, S. Argosomes: a potential vehicle for the spread of morphogens through epithelia. *Cell* 106, 633–645 (2001).

R plot code

```
library(ggplot2)

filename="Control Source"

file_t= "data\\"
file<-paste(file_t,filename, ".csv", sep="")

#data<-read.csv("FinalData\\Control Source.csv", head=TRUE, sep=",")
data<-read.csv(file, head=TRUE, sep=",")

cols<-c("#619cff", "#f8766d", "#00ba38")
#cols<-c("red", "blue", "green")

p<-ggplot(data, aes(x=data$Range, y=data$Counts, fill=data$Length)) +
  #theme_bw()+
  #theme_minimal() +
  geom_bar(width = 30, colour="black", stat="identity") +
  #geom_hline(yintercept = 2.5) +
  #geom_vline(xintercept = c(0,90,180,270)) +
  scale_fill_manual(values = cols) +
  #scale_y_discrete(drop = FALSE) +
  theme(legend.box.just = "top", legend.position = "bottom") +
  theme(panel.grid.major = element_line(colour = "gray"),
        panel.grid.minor = element_line(colour = "blue"),
        panel.background = element_blank(),
        axis.line = element_line(colour = "black"))+
  labs(title = filename,
        fill = "Length range(um)",
        y = "Cytoneme number", limits = c(0, 100), colour =
"Cylinders") +
  coord_polar(theta = "x", start=pi/2, direction=-1) +
  scale_x_discrete("", limits = c(0,90,180,270), labels =
c(0,90,180,270)) +
  scale_y_continuous(limits=c(0,5), breaks= c(1:5))
```

p